

Cite this article as: Wu Weiran, Zhou Zheng, Sun Huanzheng, et al. Dependency of Rolling Texture and Microstructure on Twinning and Recrystallization Behavior of CP-Ti Sheet[J]. Rare Metal Materials and Engineering, 2021, 50(06): 1971-1979.

ARTICLE

# Dependency of Rolling Texture and Microstructure on Twinning and Recrystallization Behavior of CP-Ti Sheet

Wu Weiran<sup>1</sup>, Zhou Zheng<sup>1</sup>, Sun Huanzheng<sup>1</sup>, Peng Lin<sup>2</sup>, Wang Ying<sup>1,2</sup>, Li Jun<sup>2</sup>, Adrien Chapuis<sup>1</sup>, Cao Huajun<sup>3</sup>, Luan Baifeng<sup>1,3</sup>

<sup>1</sup> International Joint Laboratory for Light Alloys (MOE), College of Materials Science and Engineering, Chongqing University, Chongqing 400044, China; <sup>2</sup> Pangang Group Research Institute Company, Limited, Panzhihua 617067, China; <sup>3</sup> State Key Laboratory of Mechanical Transmissions, Chongqing University, Chongqing 400044, China

**Abstract:** Commercial pure titanium (CP-Ti) sheets were cold rolled to different amounts, then annealed, and then re-rolled by 20%. Microstructure changes were investigated via electron backscatter diffraction (EBSD). After re-rolling,  $\{11\bar{2}2\} \langle \bar{1}\bar{1}23 \rangle$  contraction twins and  $\{10\bar{1}2\} \langle 10\bar{1}1 \rangle$  extension twins proliferate. A twin lamellas structure can be observed, caused by tangle of deformation twins and the generation of secondary and tertiary twins. There is no simple correlation between the average grain size and the amount of twinning. The grain size significantly decreases with the increase of pre-deformation degree, for 0.5 h annealed sample. Re-rolling tends to re-orient the lattice closer to ND. While the texture change and twin volume fraction are small and the  $\{10\bar{1}0\}$ /RD fiber remains.

**Key words:** texture; recrystallization; pure titanium; twinning

Commercially pure titanium (CP-Ti) possesses many advantages, such as low density-strength ratio, superior biocompatibility and excellent corrosion resistance<sup>[1-4]</sup>, so it has preferential applications in medical implants, heat exchangers, marine and oil industries. Commercially pure titanium owns hexagonal close-packed (hcp) structure, few easy slip systems and poor symmetry. Finally, strong deformation textures and subsequent strong mechanical anisotropy were developed.

Texture as well as chemical composition and microstructure, are significant factors for predicting, designing or selecting the material properties and deformation behavior. Strength strongly depends on the texture (i. e., crystal orientations) and the relative loading direction. Twinning, for instance, can be a firm hand in the effective design and control of texture in hcp metals<sup>[5,6]</sup>. A common observation in hcp metals is that the twin nucleation frequency and thickness of twin lamellas increases with increasing the grain size. Ghaderi and Barnett<sup>[7]</sup> show that twins span the entirety of their parent grains only when grain sizes are less than 30  $\mu\text{m}$ ; and the twin

volume fraction increases linearly with strain. Smaller grains also have lower twin volume fraction, but the number of twins is almost independent of the grain size and increases with strain<sup>[7]</sup>. In a more detailed study, Arul Kumar et al<sup>[8]</sup> found that larger grains twin earlier in the straining process because both twin nucleation and growth are easier in large grains. Also, the number of twins per grain depends more on the grain orientation and twin mode rather than the grain size.  $\{11\bar{2}1\}$  contraction twins (CTs) and  $\{10\bar{1}2\}$  extension twins (ETs) are commonly observed in titanium alloy, while secondary and tertiary twinning,  $\{11\bar{2}1\} - \{10\bar{1}2\} - \{11\bar{2}1\}$  twins, can also be observed<sup>[9]</sup>. Strain accommodation between secondary twin and matrix determines which twin variant occurs. The local stress field plays a major role in the activation of  $\{11\bar{2}2\}$  contraction twins with low Schmid factor in titanium and its alloy<sup>[10]</sup>. Variations in the grain size and grain shape may develop local stresses that are significantly different from the macroscopic stress state. Therefore, the heterogeneous microstructures of both grain size and grain

Received date: June 12, 2020

Foundation item: Chongqing University-Student Research Training Program (2017172); National Natural Science Foundation of China (51505046, 51531005, 51421001, 51371202); Fundamental Research Funds for the Central University (106112017CDJQJ138803, 2020CDJDPT001); Panxi Demonstration Project

Corresponding author: Luan Baifeng, Ph. D., Professor, College of Materials Science and Engineering, Chongqing University, Chongqing 400044, P. R. China, E-mail: bfluan@cqu.edu.cn

Copyright © 2021, Northwest Institute for Nonferrous Metal Research. Published by Science Press. All rights reserved.

orientations of parent and neighbors need to be considered together to understand the twinning behavior. Zr is another hcp metal and its prismatic slip and extensive twinning can activate at room temperature easily. In rolled hcp metals, prismatic slip generates a fiber  $\{10\bar{1}0\}$ //RD, whereas recrystallization promotes the  $\{11\bar{2}0\}$ //RD fibers generation<sup>[11,12]</sup>. In pure titanium, the texture change is caused by preferential growth of recrystallized grains<sup>[13]</sup>. It is reported that recrystallization does not change the deformed texture significantly in hcp metals<sup>[13-15]</sup>.

Most of the time, recrystallized grains have the same orientation as the deformed ones, and texture change involves the prismatic plane distribution whereas the  $\langle c \rangle$  axis distribution remains relatively unchanged<sup>[15]</sup>. Liu et al<sup>[16]</sup> investigated the recrystallization behavior of CP-Ti through reducing sheet thickness by 10%~40% followed by annealing at 550 °C for different time, and the  $\{10\bar{1}0\}$ //RD texture component was observed both after rolling and annealing. Wang et al<sup>[17]</sup> underlined that after low (20%) or medium (40%) amount of rolling, a fraction of non-TD-split basal texture is inherited from the deformed state and remains even after long time (60 min) annealing. But a strong TD-split basal texture remains both after 80% rolling and subsequent annealing. The relationship between deformed microstructure and recrystallized texture is complex. Slip and twinning are the primary deformation forms that occur in the hexagonal close-packed metals, such as titanium. Moreover, it is reported that deformation twinning is more easily activated under compressive rather than tensile stress. Therefore, it is more significant to study the dependency of rolling texture and microstructure on twinning and recrystallization behavior of CP-Ti sheet. Furthermore, those changes are the key factors to improve the subsequent performance of cold rolling and deep drawing. Thus, detailed analysis on rolling effect of twinning and recrystallization behavior was significantly necessary to establish the base for improving the deep drawability. The present experiments systematically investigated the rolling texture and microstructure dependency with twinning and recrystallization behavior of CP-Ti sheet and provided a reference for tailoring the texture in CP-Ti and optimizing the rolling process.

## 1 Experiment

Commercial pure titanium (CP-Ti) sheets with an initial thickness of 4.6 mm were received from Panzhihua Iron and Steel Research Institute. The nominal chemical composition is listed in Table 1. The as-received CP-Ti sheets were pre-cold rolled by 30%, 50% and 70% (thickness reduction ratio) with 5% in each pass, followed by annealing at 550 °C for 0.5 or 2 h in order to get full recrystallization. Then all the annealed CP-Ti samples were cold re-rolled by 20% with the same

**Table 1 Nominal chemical composition of CP-Ti (wt%)**

Fe	O	C	N	Ti
0.04	0.04	0.01	0.003	Bal.

process as primary rolling. A scanning electron microscope (TESCAN MIRA3) equipped with electron backscatter diffraction detector was used to observe the microstructure of annealed CP-Ti samples as well as the re-rolled samples. Scanning step size of 0.3 μm was adopted for all samples. The EBSD data were collected on a 150 μm×150 μm area on a surface containing the rolling direction (RD) and the normal direction (ND), and the data were processed and analyzed with Channel 5 software from HKL Technology.

## 2 Results and Discussion

### 2.1 Microstructure of initial material

Fig. 1 shows the orientation imaging map, pole figure and misorientation angle distribution histogram of the initial material. The initial material was hot rolled and annealed, and has an average grain size of 6.5 μm. It can be observed from inverse pole figure (IPF) map and band contrast map that there is no twin in the initial CP-Ti sheets. The pole figure in Fig. 1c shows that the initial material has a typical bimodal TD split basal texture. The histogram of the initial material's misorientation angle distribution (MAD) shows that the percentage of low angle grain boundary (LAGB) is 8.4%, which means that most of the grain boundaries are high angle grain boundaries (HAGBs), and the distribution of grain boundaries is homogeneous.

### 2.2 Microstructure of the annealed and re-rolled material

Fig. 2 and Fig. 3 show the microstructures of the six samples rolled by 30%, 50% and 70% followed by annealing for 0.5 and 2 h, respectively. In all six pre-deformed samples,  $\{11\bar{2}2\} \langle \bar{1}\bar{1}23 \rangle$  contraction twinning and  $\{10\bar{1}2\} \langle 10\bar{1}1 \rangle$  extension twinning are activated<sup>[16,17]</sup>, which are indicated by blue and red lines in the image quality (IQ) maps, respectively. It can be seen that the twins almost totally disappear during annealing. Rolling deformation introduces various defects and promotes nucleation during recrystallization, which results in the refinement of grain.

Fig. 4 and Fig. 5 show the EBSD IPF maps and band contrast maps of the 20% re-rolled CP-Ti sheets, which were processed in primary rolling by 30%, 50% and 70% pre-deformation and then annealed for 0.5 and 2 h at 550 °C. All map shows fully recrystallized microstructure, except the 30%-0.5 h sample, which exhibits some deformed and recovered areas.

Comparing the image quality maps after re-rolling (Fig. 4) with the former processed sample (Fig. 2 and Fig. 3), the amount of twins and twin-like boundaries increases sharply, which means that  $\{11\bar{2}2\} \langle \bar{1}\bar{1}23 \rangle$  contraction twinning and  $\{10\bar{1}2\} \langle 10\bar{1}1 \rangle$  extension twinning are largely activated during re-rolling. According to the previous study<sup>[16]</sup>, the fraction of twin boundary is the maximal at 20% rolling, and the boundary of twin-matrix characteristic is destroyed by lattice rotation and dislocation accumulation in the further rolling. It can be observed that sometimes both extension and compression twins coexist in a single grain.

### 2.3 Texture evolution of the material

Fig. 6 displays EBSD  $\{0001\}$  and  $\{10\bar{1}0\}$  pole figures of the

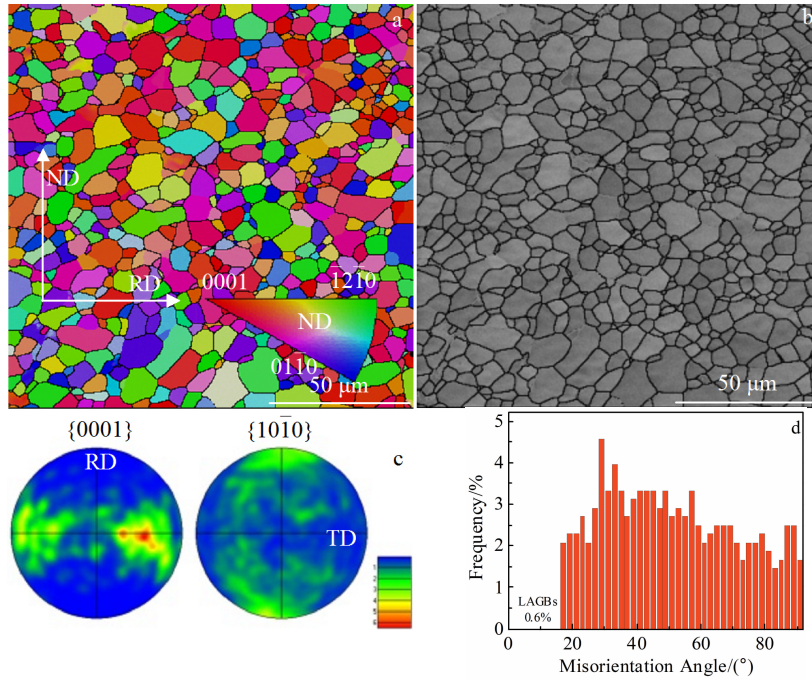


Fig.1 IPF map (a), band contrast map (b), pole figures (c), and misorientation angle distribution (d) of initial CP-Ti material

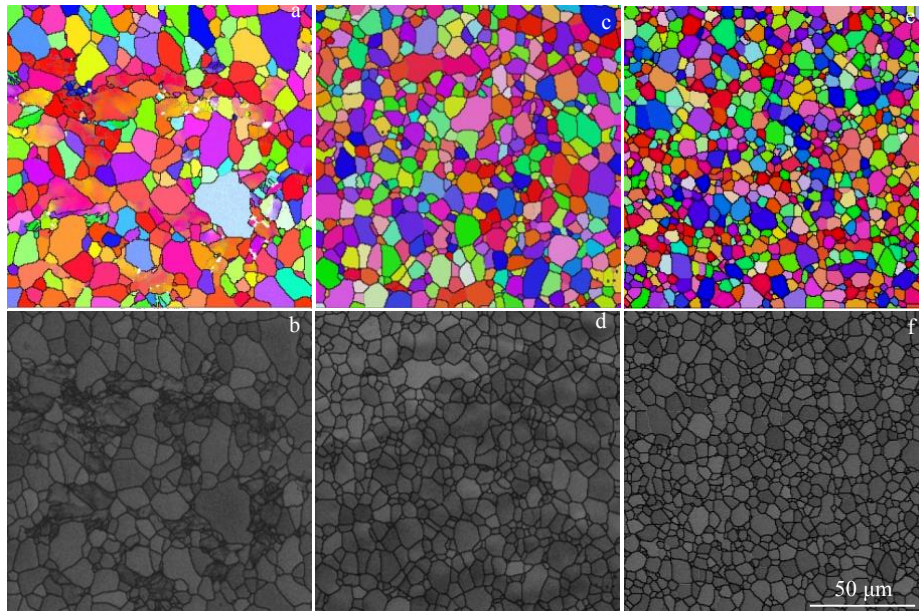


Fig.2 IPF maps (a, c, e) and band contrast maps (b, d, f) of CP-Ti sheets after annealing at 550 °C for 0.5 h with various primary deformation: (a, b) 30%, (c, d) 50%, and (e, f) 70%

samples annealed for 0.5 h after primary rolling to various deformation (30%, 50%, 70%) and their pole figures after 20% re-rolling. Fig. 7 shows the corresponding RD and TD inverse pole figures. All of the CP-Ti sheets have a typical TD-split basal texture. The spread of texture of the annealed sheets is remarkably larger than that after 20% re-rolling, so re-rolling increases the intensity of the main TD-split basal texture.

The RD inverse pole figures clearly show that re-rolling process increases the intensity of  $\{10\bar{1}0\}$ //RD texture fiber in all samples, and the intensity of texture of all tested samples decreases with increasing the primary cold rolling. This texture feature attributes to a higher degree of recrystallization during the identical heat treatment process induced by the large deformation, which is consistent with the results that

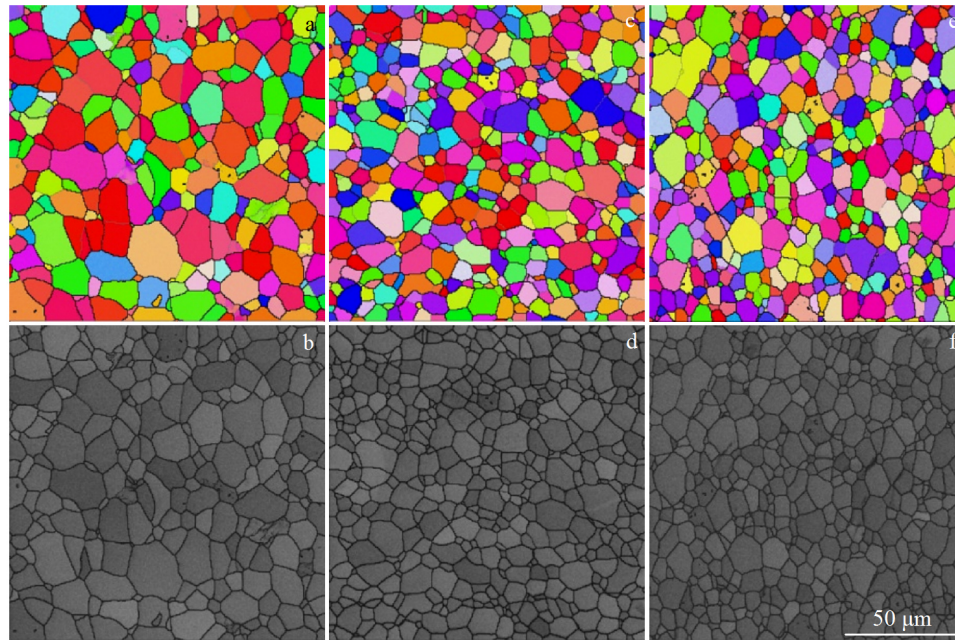


Fig.3 EBSD IPF maps (a, c, e) and band contrast maps (b, d, f) of CP-Ti sheets after annealing at 550 °C for 2 h with various primary deformation: (a, b) 30%, (c, d) 50%, and (e, f) 70%

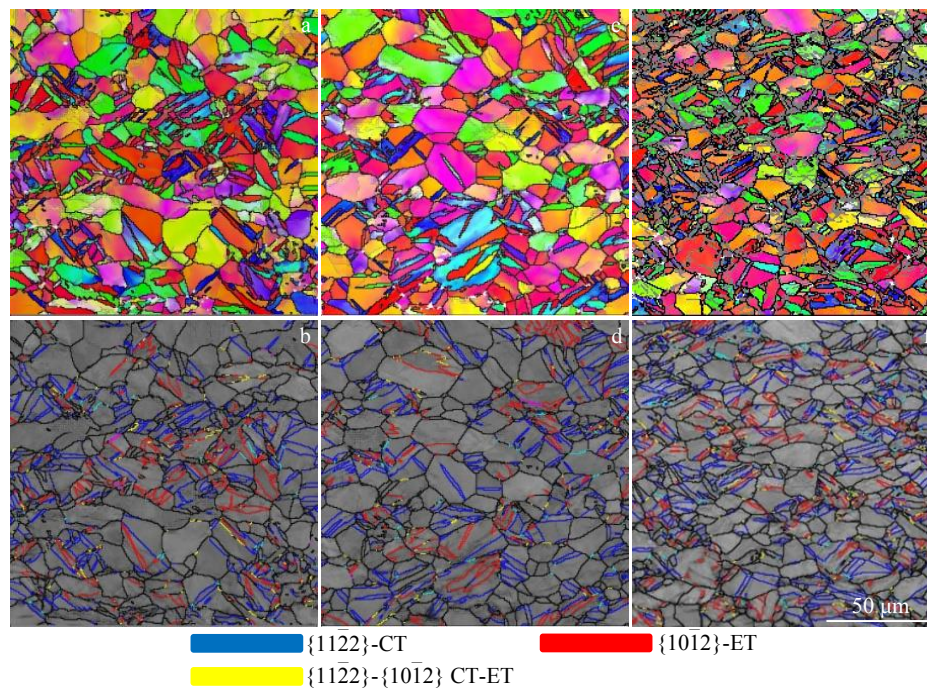


Fig.4 EBSD IPF maps (a, c, e) and band contrast maps (b, d, f) of 20% re-rolled CP-Ti sheets after annealing at 550 °C for 0.5 h with various primary cold rolling deformations: (a, b) 30%, (c, d) 50%, and (e, f) 70%

discussed in Section 2.1. In addition, re-rolling tilt the  $c$ -axis of crystal less toward TD, which is more visible in the TD-IPF than in the (0001) pole figures.

Fig.8 and Fig.9 show the  $\{0001\}$ ,  $\{10\bar{1}0\}$  pole figures and

RD, TD inverse pole figures of the CP-Ti sheets annealed for 2 h and the 20% cold re-rolled sheets with primary cold rolling of 30%, 50% and 70%. Similar to the sheets annealed for 0.5 h in Fig.7, all the CP-Ti sheets annealed for 2 h and

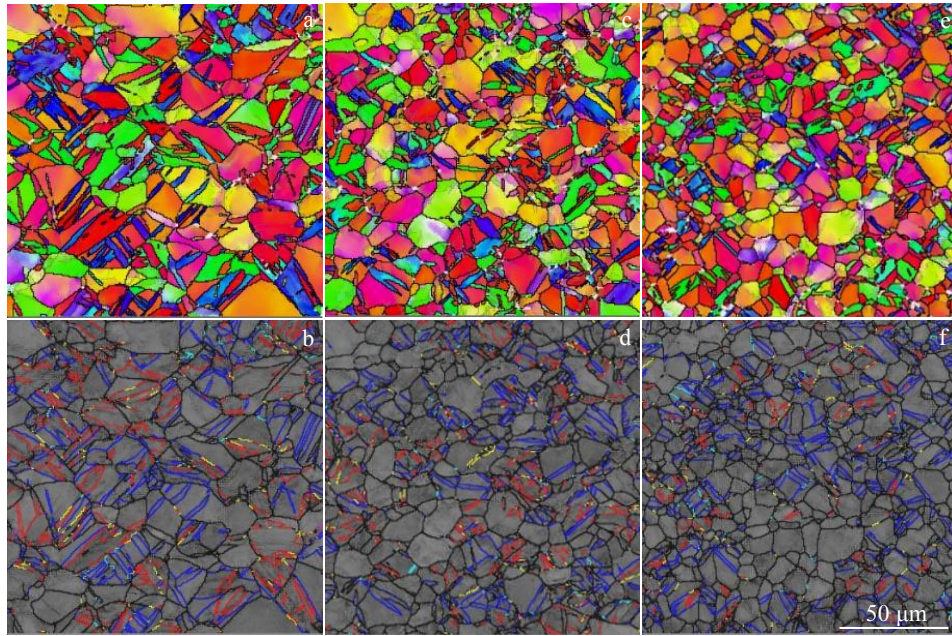


Fig.5 IPF maps (a, c, e) and band contrast maps (b, d, f) of 20% re-rolled CP-Ti sheets after annealing at 550 °C for 2 h with various primary cold rolling deformations: (a, b) 30%, (c, d) 50%, and (e, f) 70%

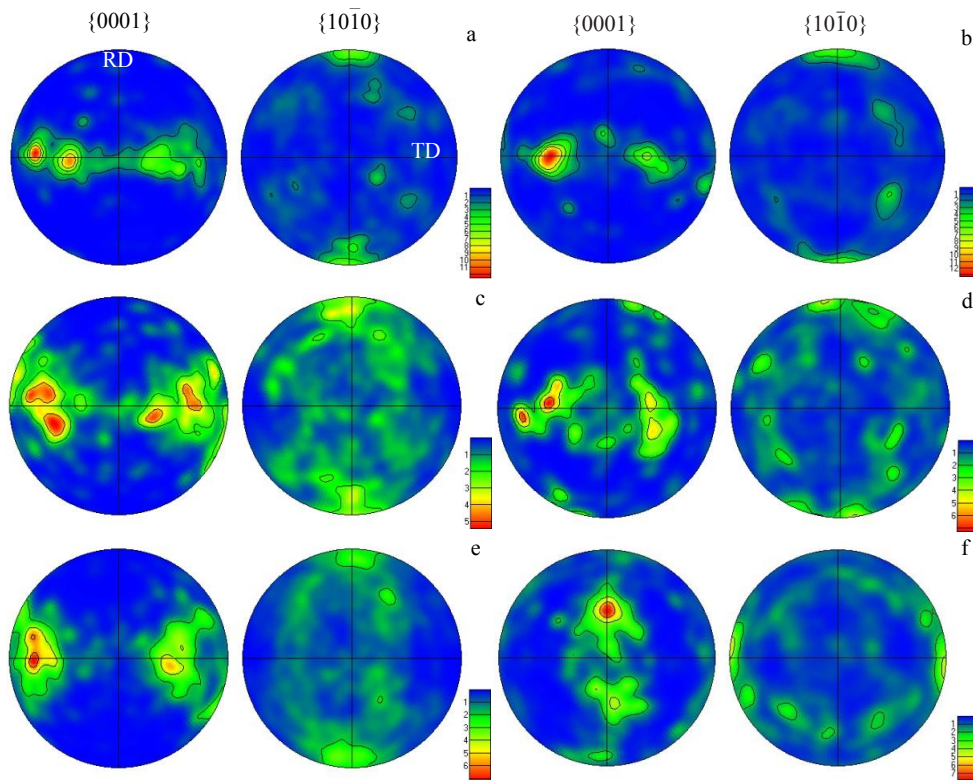


Fig.6 {0001} and {10 $\bar{1}0$ } pole figures of treated CP-Ti sheets after primary cold rolling+annealing+re-rolling deformation: (a) 30%+550 °C/0.5 h, (b) 30%+550 °C/0.5 h+20%, (c) 50%+550 °C/0.5 h, (d) 50%+550 °C/0.5 h+20%, (e) 70%+550 °C/0.5 h, and (f) 70%+550 °C/0.5 h+20%

their re-rolled pole figures have the typical TD-split basal texture, and the {10 $\bar{1}0$ }/RD fiber is stronger for low pre-

rolling. Compared with the 0.5 h annealed samples, the spread of orientation intensity in pole figures of the re-rolled ones is

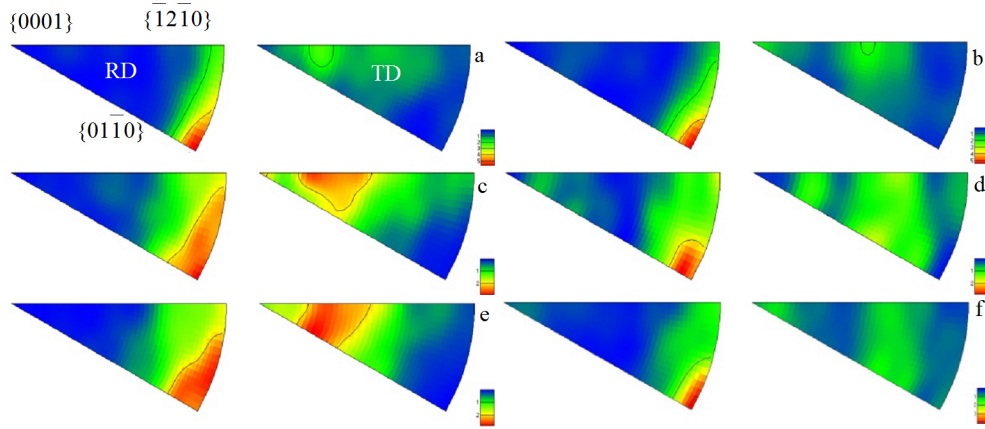


Fig.7 IPFs along RD and TD of treated CP-Ti sheets after primary rolling+annealing+re-rolling deformation: (a) 30%+550 °C/0.5 h, (b) 30%+550 °C/0.5 h+20%, (c) 50%+550 °C/0.5 h, (d) 50%+550 °C/0.5 h+20%, (e) 70%+550 °C/0.5 h, and (f) 70%+550 °C/0.5 h+20%

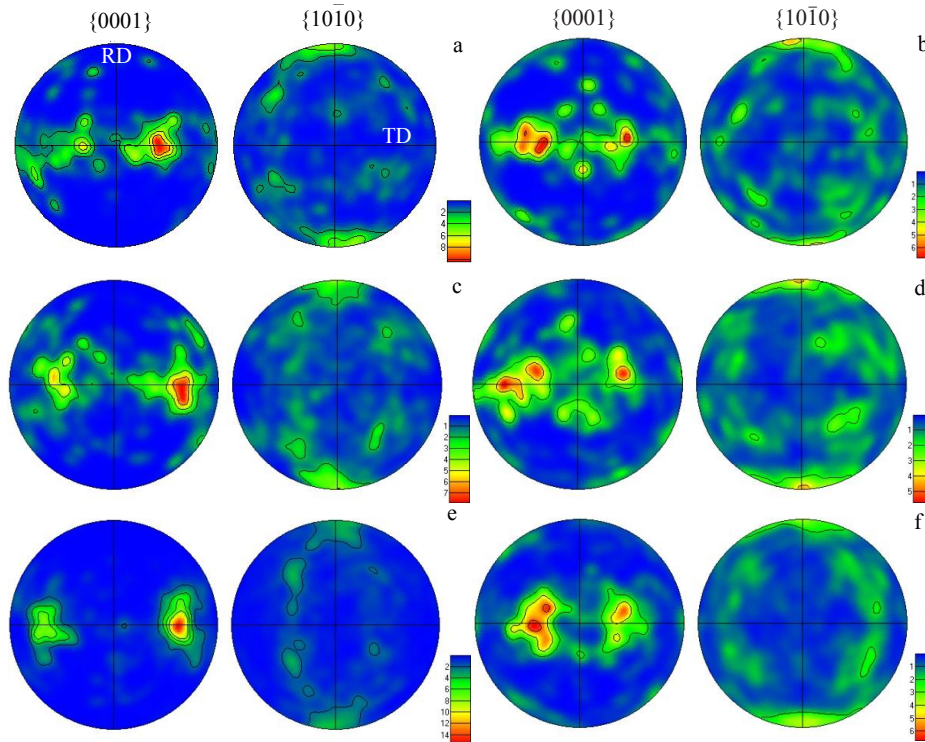


Fig.8 {0001} and {1010} pole figures of treated CP-Ti sheets after primary cold rolling+annealing+re-rolling deformation: (a) 30%+550 °C/2 h, (b) 30%+550 °C/2 h+20%, (c) 50%+550 °C/2 h, (d) 50%+550 °C/2 h+20%, (e) 70%+550 °C/2 h, and (f) 70%+550 °C/2 h+20%

larger than that of the only annealed samples. The only annealed sheets' orientation intensities are slightly higher than the re-rolled ones. The RD inverse pole figures shows that the peaks of orientation density are near  $\langle 01\bar{1}0 \rangle$  for all tested samples.

The misorientation angle distribution (MAD) of the re-rolled samples is shown in Fig. 10. Grain boundaries with misorientations lower and higher than 15° are denoted as low

angle grain boundaries (LAGBs) and high angle grain boundaries (HAGBs), respectively. The LAGBs value is derived from the result of misorientation angle distribution that was processed by Channel 5 software. It is worth noting that the sharp peaks at approximately 64° and 85° are caused by  $\{11\bar{2}2\}$  contraction twin and  $\{10\bar{1}2\}$  extension twin boundaries, respectively. In the MAD map of all the six re-rolled CP-Ti sheets, the highest peak near 64° suggests that con-

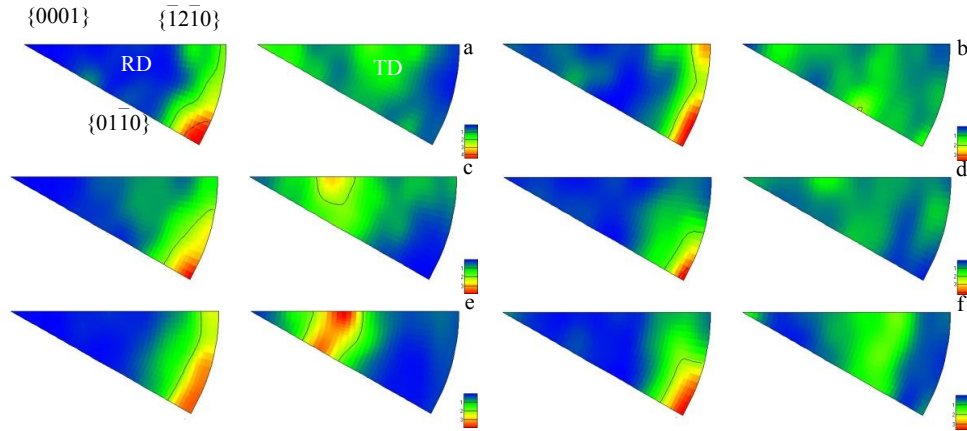


Fig.9 Inverse pole figures of treated CP-Ti sheets after primary cold rolling+annealing+re-rolling deformation: (a) 30%+550 °C/2 h, (b) 30%+550 °C/2 h+20%, (c) 50%+550 °C/2 h, (d) 50%+550 °C/2 h+20%, (e) 70%+550 °C/2 h, and (f) 70%+550 °C/2 h+20%

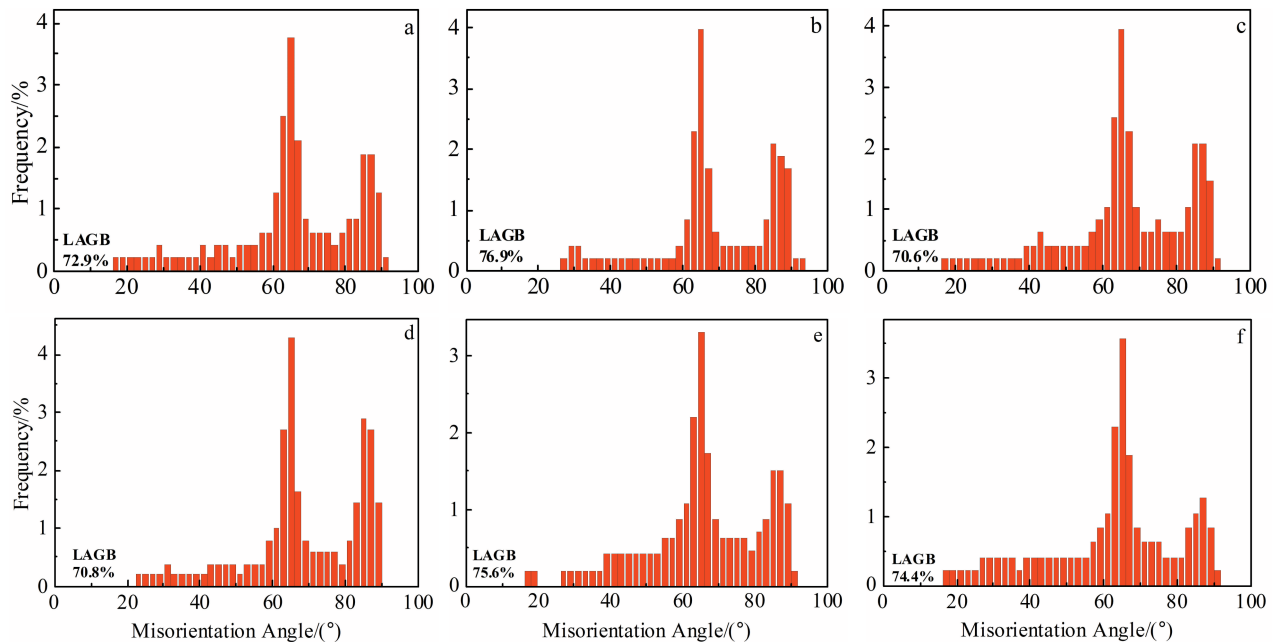


Fig.10 Misorientation angle distributions of the 20% re-rolled samples after various initial rolling deformations and annealing : (a) 30%+550 °C/0.5 h+20%, (b) 50%+550 °C/0.5 h+20%, (c) 70%+550 °C/0.5 h+20%, (d) 30%+550 °C/2 h+20%, (e) 50%+550 °C/2 h+20%, and (f) 70%+550 °C/2 h+20%

traction twinning is predominant.

Twin area fraction statistics of the sheets during 20% re-rolling after different deformation and annealing are given in Fig. 11. Twin area fraction is measured by the proportion of red ( $85^\circ < 11\bar{2}0 \rangle$ ) or blue lines ( $64^\circ < 10\bar{1}0 \rangle$ ) to the overall investigated area using Channel 5 software based on twin boundary criterion. Twin boundary criterion means that only regions that surrounded by a twin boundary are identified as twins. Measurements of the twin area fraction in Fig. 4 and 5 show a strong twin volume fraction dependency with initial

texture. As suggested by the misorientation angle distribution, contraction twins are predominated. For samples with annealing for 0.5 h after primary rolling, the fraction of contraction twinning and extension twinning slightly fluctuates with the change of primary rolling fraction. This is in sharp contrast to that of the re-rolled sheets for samples annealed for 2 h, which means that the extension twin volume fraction decreases with initial rolling strain, whereas the volume fraction of compression twin is minimum for 50% pre-rolling samples.

The grain size for different samples is shown in Fig. 12. As

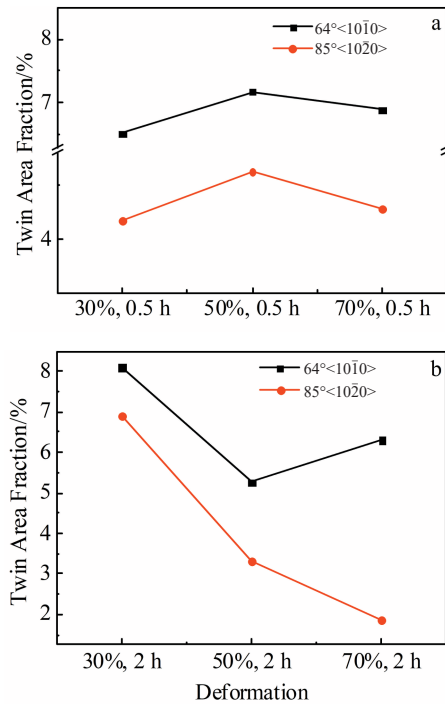


Fig.11 Twin area fraction evolution during 20% re-rolling after different deformation and annealing for 0.5 h (a) and 2 h (b)

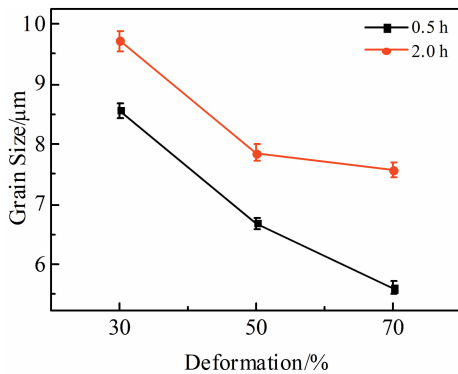


Fig.12 Grain size of annealed samples after pre-rolling to various deformations

illustrated, grain size increases with the annealing time, so the grain sizes of the CP-Ti sheets that are annealed at 550 °C for 2 h are all higher than that of the 0.5 h annealed sheets with the same deformation. The grain size decreases with increasing the pre-deformation fraction because the higher pre-deformation promotes recrystallization nucleation, thus resulting in the smaller grains. The fact is that there is no correlation between the grain size and the number of twins, supporting the conclusions of Ghaderi and Barnett<sup>[7]</sup>.

The mechanical properties are simply evaluated through hardness test. As shown in Fig. 13, the hardness of the re-rolled samples is significantly higher than the ones before re-

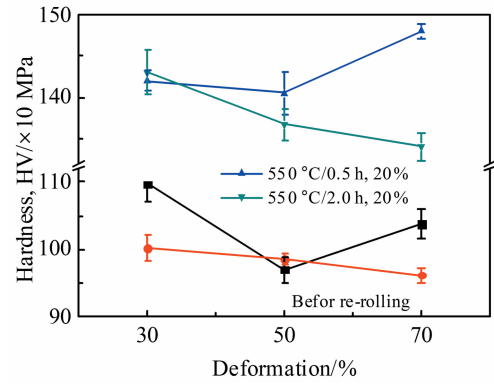


Fig.13 Hardness of sheets in groups with annealing for different time before and after 20% re-rolling

rolling because of the introduction of dislocations. The hardness of the material that is annealed for 2 h decreases with the increase of pre-rolling, which is not coherent with the vary tendency of grain size. According to Hall-Petch relationship, the hardness should increase with decreasing the grain size, so some other factors should explain the hardness tendency. The hardness is clearly not dictated by the grain size. The 30%+550 °C/0.5 h and 30%+550 °C/0.5 h+20% may be relatively harder because partially unrecrystallized microstructure exists. So, for the material annealed for 0.5 h, the hardness increases with decreasing the grain size.

### 3 Conclusions

- 1) The grain size significantly decreases with the increase of pre-deformation, approximately linearly, and this decrease is sharper for 0.5 h annealing than 2 h annealing at 550 °C.
- 2) Re-rolling can change the grain orientation and texture by tilting more TD-split basal textures off TD, so the lattice  $c$ -axis is closer to ND.
- 3) Measurements of the twin area fraction show a strong twin volume fraction dependency with initial texture. The texture evolution after re-rolling is minor with  $\sim 10\%$  twin volume fraction, and the  $\{10\bar{1}0\}$ //RD fiber remains in particular.

### References

- 1 LÜJERING G, WILLIAMS J C. *Titanium*, 2nd ed[M]. New York: Springer, 2007: 1
- 2 NASIRI-ABARBOKOH H, EKRAMI A, ZIAEI-MOAYYED A A. *Material Design*[J], 2013, 44: 528
- 3 HUANG W, WANG Y, LI Z R *et al.* *Chinese Journal of Nonferrous Metals*[J], 2008, 18(8): 1440 (in Chinese)
- 4 PACHLA W, KULCZYK M, SUS-RYSZKOWSKA M *et al.* *Journal of Materials Processing Technology*[J], 2008, 205(1-3): 173
- 5 XIN Y C, WANG M Y, ZENG Z *et al.* *Scripta Materialia*[J], 2011, 64(10): 986
- 6 XIN Y C, ZHOU H, YU H H *et al.* *Materials Science and*

- Engineering A*[J], 2015, 622: 178
- 7 Ghaderi A, Barnett M R. *Acta Materialia*[J], 2011, 59(20): 7824
- 8 Arul Kumar M, Wroński M, McCabe R J et al. *Acta Materialia* [J], 2018, 148: 123
- 9 Qin H, Jonas J J. *Acta Materialia*[J], 2014, 75: 198
- 10 Guo Y, Abdolvand H, Britton T B et al. *Acta Materialia*[J], 2017, 126: 221
- 11 Honniball P D, Preuss M, Rugg D et al. *Metallurgical and Materials Transactions A*[J], 2015, 46(5): 2143
- 12 Isaenkova G, Perlovich Yu A, Fesenko V A et al. *The Physics of Metals and Metallography*[J], 2014, 115(8): 756
- 13 Bozzolo N, Dewobroto N, Grosdidier T et al. *Materials Science and Engineering A*[J], 2005, 397(1-2): 346
- 14 Pérez-Prado M T, Ruano O A. *Scripta Materialia*[J], 2002, 46(2): 149
- 15 Gerspach F, Bozzolo N, Wagner F. *Scripta Materialia*[J], 2009, 60(4): 203
- 16 Liu N, Wang Y, He W J et al. *Transactions Nonferrous Metals Society of China*[J], 2018, 28: 1123
- 17 Wang Y, He W J, Liu N et al. *Materials Characterization*[J], 2018, 136: 1

## 工业纯钛板材的轧制织构及微观组织对其孪晶和再结晶行为的依赖性

吴蔚然<sup>1</sup>, 周正<sup>1</sup>, 孙焕政<sup>1</sup>, 彭琳<sup>2</sup>, 王莹<sup>1,2</sup>, 李军<sup>2</sup>, Adrien Chapuis<sup>1</sup>, 曹华军<sup>3</sup>, 栾佰峰<sup>1,3</sup>

(1. 重庆大学材料科学与工程学院 国际轻合金联合实验室 (MOE), 重庆 400044)

(2. 攀钢集团研究院有限公司, 四川攀枝花 617067)

(3. 重庆大学机械传动国家重点实验室, 重庆 400044)

**摘要:** 将工业纯钛 (CP-Ti) 板轧制至不同程度, 随后进行退火以及进行 20% 的再轧制。通过电子背散射衍射 (EBSD) 对合金微观组织的变化进行表征。重新轧制后,  $\{11\bar{2}2\} \langle \bar{1}\bar{1}23 \rangle$  压缩孪晶和  $\{10\bar{1}2\} \langle 10\bar{1}1 \rangle$  拉伸孪晶产生。可以观察到孪晶的层状结构, 这是由变形孪晶的缠结以及二次和三次孪晶的产生引起的。平均晶粒尺寸和孪晶量之间没有简单的关联。0.5 h 退火样品中的晶粒尺寸随其预变形程度的增加而显著减小。重新轧制倾向于使晶格的重新取向更接近法线方向。虽然织构变化和孪晶体积分数很小, 但平行于 RD 方向的  $\{10\bar{1}0\}$  纤维织构仍然保留。

**关键词:** 织构; 再结晶; 工业纯钛; 孪晶

作者简介: 吴蔚然, 女, 1997年生, 硕士生, 重庆大学材料科学与工程学院, 重庆 400044, E-mail: 20155487@cqu.edu.cn